

IN-SITU IMAGE PROCESSING OF FATIGUE DAMAGED CROSS-PLY LAMINATES COUPLED WITH SIMULATION TO PREDICT RESIDUAL STRENGTH DEGRADATION

Miloš Drašković¹, Anthony Pickett¹ and Peter Middendorf³

¹Institute of Aircraft Design, University of Stuttgart, Pfaffenwaldring 31, 70569 Stuttgart, Germany
Email: draskovic@ifb.uni-stuttgart.de Web Page: <http://www.ifb.uni-stuttgart.de>

Keywords: composites, image processing, residual strength, fatigue, XFEM

1 Abstract

A novel experimental method for residual strength testing of Glass Fibre Reinforced Polymer (GFRP) composite materials based on image processing and automated virtual testing is presented with the goal to significantly reduce fatigue-testing time for composite materials. In this paper the generation and development of cracks is detected in-situ, using an optical measurement system, which can map the position and shape of cracks. The detected crack geometry is recognized and automatically translated into a Finite Element (FE) idealisation in order to create a mesoscopic virtual specimen with discrete damage to predict residual strength. The novelty of the methodology presented is to use the damage state of a composite material in order to enable an automated characterization process. Using a combination of experiment and virtual testing it is possible to describe the residual strength curve with significantly less specimens compared to physical testing. To fulfil this task, a camera system is used to acquire in-situ images of the specimen during a fatigue test. The geometry of cracks, as well as their relative location is then extracted, using an image-processing algorithm and thereafter transferred into an FE simulation for virtual testing.

2 Introduction

The use of Fibre-Reinforced Polymer (FRP) composite materials is increasing in many engineering applications. Along with this increased use, the need for better understanding of their mechanical behaviour over extended periods is becoming more essential. Full characterization of this long-term fatigue behaviour requires extensive material and prototype testing, which results with great investments of time and resources. To ensure safe designs, current lifetime prediction methodologies use large factors of safety resulting in overdesigned and unnecessarily heavy composite structures.

2.1 Fatigue life characterization of composite materials

Compared to metallic materials, where the mechanisms that influence the fatigue life are well understood, composite materials have a complex fatigue behaviour. In metallic materials, small microcracks gradually grow and coalesce to form a dominant crack leading to final failure. In anisotropic composite materials fatigue damage is a complex process that involves different types of damage at different length-scales including matrix cracking, fibre-breakage, delamination and interface failure. These types of damage occur independently and, at a later stage in the lifetime of a composite structure will also interact. Thus increasing the complexity of the problem at hand, as these interactions are difficult to describe.

The degree of damage in a composite material can be determined by measuring the degradation of a parameter or a metric, which is relevant to a particular damage mode. This can usually be degradation of stiffness or strength. Degrieck and Van Paepegem [1] give an excellent review on fatigue-life modelling, where models are classified into three categories, namely, fatigue life models, phenomenological models for residual stiffness/strength and progressive damage models. These models introduce one or more chosen damage variables in order to describe the degradation of composite laminates using damage mechanisms as their basis. This degradation is then correlated to damage growth using residual mechanical properties.

2.2 Residual strength degradation

Residual strength theory assumes that damage accumulates until the bearing load of a composite material is lower than the maximum cyclic stress level applied to the structure. The relative simplicity of these models as a “natural failure criteria” is when residual strength becomes equal to, or falls below the applied stress, and constitutes material failure. This offers an easy to understand framework for the designer. Compared to damage accumulation models, residual strength models have the advantage that they can be easily fitted to intermediate points during fatigue lifetime, because damage is evaluated in terms of a physical quantity, which is residual strength. [2] These models commonly use the Strength-Life Equal Rank Approach (SLERA) [3] in order to connect the distribution of static strength to the distribution of fatigue life. SLERA states that strength and life ranks are correlated. This means that specimens with a high initial static strength should have a longer lifetime compared to specimens with a low initial static strength. One disadvantage of this method is that it is not possible to confirm the hypothesis experimentally, because both the static strength measurement and fatigue life measurement are destructive tests and it is not possible to test the same specimen twice. An excellent review of different residual strength degradation models can be found in Post et al. ([4], [5]). A couple of models from this review are presented below:

Broutman and Sahu have presented one of the earliest residual strength models:

$$\sigma_r = \sigma_{ult} - \sum_i (\sigma_{ult} - \sigma_p^i) \left(\frac{n_i}{N_i} \right) \quad (1)$$

They have shown this model yields results that are more accurate than the linear Palmgren-Miner damage accumulation.

Schaff and Davidson [6] proposed the following equation for evolution of residual strength:

$$\sigma_r = \sigma_{ult} - (\sigma_{ult} - \sigma_a) \left(\frac{n}{N} \right)^C \quad (2)$$

where C is assumed to vary with the magnitude of σ_a and the R-ratio. In order to determine C a heuristic approach is necessary and the value must be determined from residual strength tests.

Nijssen [7] has described the following testing conditions required for a thorough determination of C :

- The test spectrum should cover representative fatigue regimes (tension-tension, compression-tension and tension-compression fatigue).
- Residual strength testing should be carried out at both high cycle and low cycle fatigue.
- Different R-values are required for residual strength testing.

- A sufficient number of specimens at each entry in the test matrix is necessary to obtain statistically viable and interpretable results.

According to Vassilopoulos [8] the residual strength theory has some drawbacks:

- Remaining fatigue life cannot be assessed with Non-Destructive Test (NDT) methods, because specimen failure is required in order to derive an expression for damage.
- Residual strength changes very slowly until close to failure (“sudden death”).
- Extensive experimental work is necessary in order to establish a residual strength database.

The aim of this study is to address the issue of extensive experimentation using virtual testing in order to facilitate the residual strength approach. This is done by combining real fatigue experiments with virtual residual-strength analyses giving a methodology that should be able to significantly reduce the required number of test specimens.

3 The methodology – automated virtual residual strength testing

The main drawback of the residual-strength method is that many specimens must be tested in order to predict fatigue life for a composite structure. A minimum of five specimens per lifetime fraction is recommended with five lifetime fractions to be used. After each lifetime fraction, the specimens have to be statically loaded to failure. This is the second drawback of this method, since repeatability of the tests is non-existent, that is, one cannot test a specimen to failure more than once. At least three stress levels should be considered for this characterization (one for high cycle fatigue, one for low cycle fatigue and one intermediary stress level); resulting in a minimum of 75 specimens to be tested.

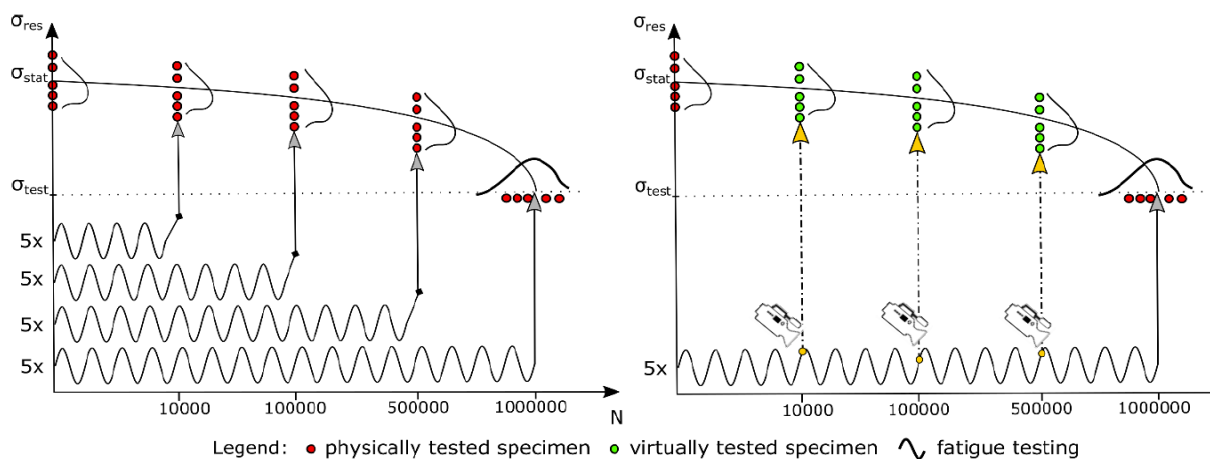


Figure 1 A comparison between state of the art residual strength testing and the proposed virtual testing methodology

Until recently, the determination of damage of a specimen, for use as input for progressive damage modelling has been a strenuous task to determine experimentally, since intra-laminar cracks had to be counted manually in order to determine crack density metrics. The subjectivity of this type of test, as well as the labour intensity associated with it, has led to fewer experimental campaigns and significant parametrisation of data resulting in conclusions that are difficult to confirm. Glud et al. [9] have developed an automated crack counting system which counts the cracks in a GFRP specimen by recording the front of the specimen.

The novelty of the methodology presented is to use the damage state of a composite material in order to enable a faster, more efficient and automated characterization. On the right-hand side of Figure 1 it is shown that using a combination of experiment and virtual testing it is possible to describe the residual

strength curve with only five specimens, compared to 25 specimens on the left-hand side, thereby significantly reducing testing effort and time.

In order to fulfil this task, a camera system is used to acquire in-situ images of the specimen face and sides during a fatigue test. The geometry of cracks, as well as their relative location are then extracted, using an image-processing algorithm. This algorithm uses pattern recognition for correct filtering of the crack geometry. The crack geometry is then analysed and simplified so that it can be automatically transferred to a finite element model for analysis. Figure 2 shows the process setup of acquiring cracks of a specimen and transferring these cracks into ABAQUS for FE analysis.

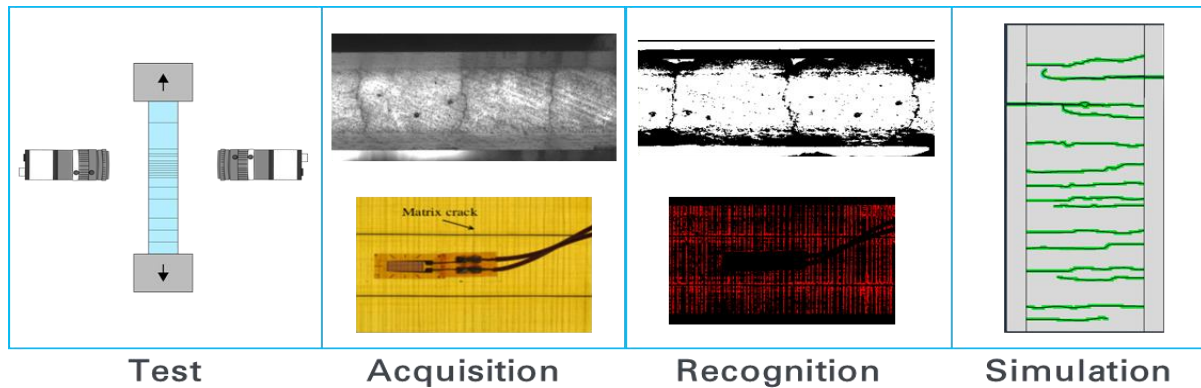


Figure 2 Experimental procedure of crack extraction, image processing and automated finite element modelling. From left to right: acquisition of cracks with a camera system, side view of a crack shape and a face view of transverse cracks, crack geometry extraction through image processing, automatically generated FEM model.

4 Experimentation

The experimental setup consists of a camera system integrated with a fatigue-testing machine. After inserting a specimen into the testing machine, the first images are acquired. The specimen is then cyclic loaded in tension-tension for a predefined number of cycles, followed by a low-level tensile loading that facilitates opening of the cracks, enabling the system to visualise as many cracks as possible. The testing-machine triggers the imaging system, which takes images of the cracked specimen. After the images have been acquired, they are prepared for further processing and the cyclic loading continues up to the next predefined number of cycles.

4.1 In-situ optical measurement system

The in-situ optical measurement system consists of three cameras, two of which are placed so that the sides of the specimen can be visualised. A third camera visualises the specimen face. Based on earlier internal experimentation with different cameras, a compromise between a good resolution and frame rate has been achieved by using IDS UEye RGB cameras with a square 1-inch sensor incorporating a resolution of 5 Megapixels. The frame-rate of 60 frames per second is high enough for a continuous acquisition of images throughout the loading cycles, which enables the constant tracking of crack development during the test. The trigger-box for the measurement system is a fully customized solution, which enables the use of up to 12 high-power LEDs, which can be controlled independently using a custom software solution. Figure 3 depicts the measurement system.

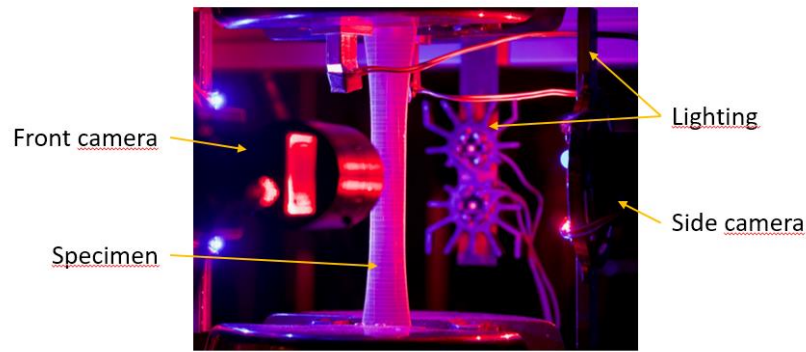


Figure 3 The experimental setup

4.2 Specimen fabrication

Two different GFRP materials, namely, a quasi unidirectional textile E-Glass (Interglas 92145) with 5% weft yarn and a prepreg material (Hexcel UD600/G HexPly M9.6GF) with $[0_n/90_m]_s$ layup were tested showing significant differences in the cracking process. The test platens for the textile material were made using the Vacuum assisted processing (VAP[®]), yielding platens with very low void content. This process is similar to Vacuum Assisted Resin Infusion (VARI) with the difference that the VAP process uses an additional semi-permeable membrane that stops the resin from flowing out while simultaneously allowing excess air to flow through the membrane. For these specimens an epoxy resin RIMR135 and RIMH1366 curing agent from Hexion was used. This combination of materials enabled a glass-like transparency of the specimens, allowing better visualisation of cracks. Prepreg specimens have shown a lower transparency compared to the textile specimens. A comparison of specimen transparency between the textile and prepreg specimens is shown in the left side of Figure 4.

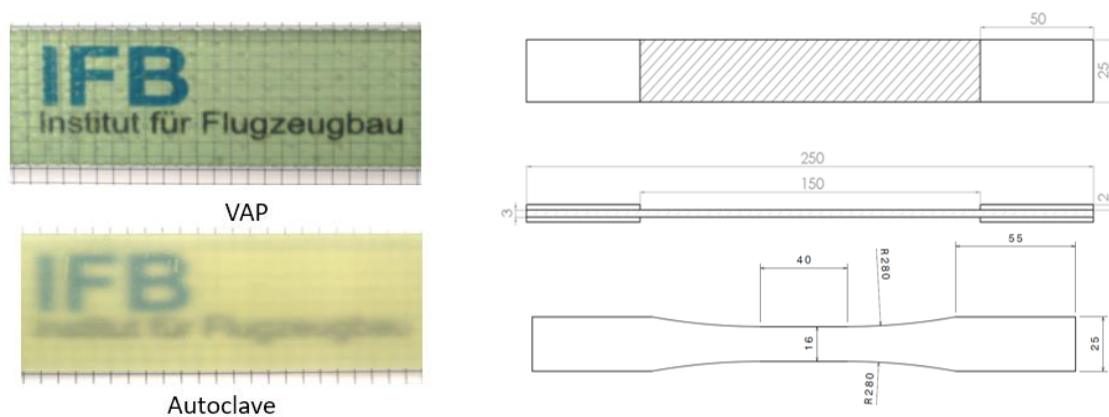


Figure 4 from left to right: transparency comparison of VAP vs Autoclave processing, Specimen dimensions flat vs dog-bone shaped specimen

Specimen geometry based on the DIN EN ISO 527-4 test standard was chosen for fatigue testing. The dimensions of the specimen are shown in the right side of Figure 4. The specimens were cut out of GFRP plates with a diamond circular saw. It should be noted that the surface quality of specimen edges after cutting with a diamond saw was not good enough for visualisation of small cracks. Therefore, a grinding process was developed which enabled a surface quality of the edges similar to a typical micrography polishing process. For this process, a Struers Tegramin grinding machine was used with a specially developed fixture, which enables the operator to hold the specimen in place. During the optimization of this process, similar surface quality was achieved with a 4000 Grit grinding plate and the standard micrography grinding process, with only 5 minutes per specimen side for the grinding plate method compared to 20 minutes per specimen side using the standard micrography polishing process.

Since the optical system has a finite field of view (FOV=60x60mm), which is smaller than the specimen free length, it was decided to use a dog-bone shaped specimen. The geometry of the dog-bone specimen is presented in Figure 4. This specimen enables the system to observe the smallest cross-section over a gauge length of 50mm thus enabling the measurement system to remain stationary, which enables calibration of the system and keeps the system costs and complexity to a minimum. For this type of specimen, a CNC Router has been modified to enable the fabrication of final geometry with a surface quality to match that of a polished specimen.

4.3 Image processing of cracked specimens

The purpose of using digital image processing tools is not only to decrease the time and cost of the experimental procedure, but also to minimize the subjective influence of the experimenter during the crack counting process. The process starts with image acquisition and continues with image-processing by using modules from a Python based image-processing package Scikit-image [10] in order to prepare the image for automated crack tracing. The acquired image is converted into an 8-bit grayscale image and subsequently with a thresholding algorithm [11] converted into a black and white binary image where value 1 represents white and value 0 black. Afterwards, morphological operators are used to thin the crack geometry enabling a skeletal image of the cracked specimen to be obtained. With this image, it is possible to identify the branching points as well as the endpoints of the cracks. A crack-tracing algorithm traces the contours of the binary crack images where non-zero values belong to cracks, and zero values belong to the background. After the cracks have been traced, they are simplified using an iterative polygonal approximation algorithm by Ramer [12]. Figure 5 depicts this process.

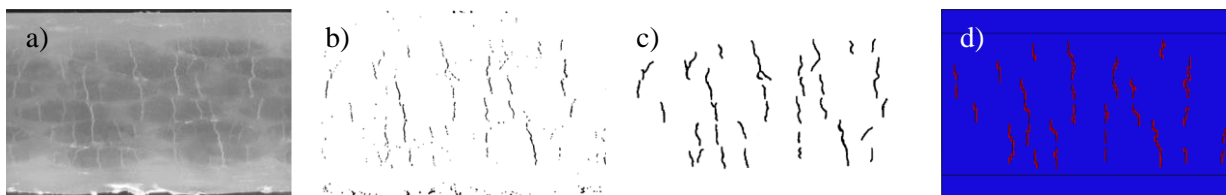


Figure 5 a) in-situ image of a specimen, b) processed image, c) enhanced image, d) automatically generated model in ABAQUS

4.4 Virtual residual strength testing

After crack image identification, the crack locations, together with critical point locations, are automatically transferred into ABAQUS using a python script. A 2D plane containing the crack geometry is generated and automatically meshed. Mesh settings can be defined in the python script that can result in either an unstructured mesh where a crack is defined as a partition, or a structured mesh where the crack is defined as a seam. Using this model, a virtual tensile test is then carried out in order to determine the residual strength of the specimen.

5 Results

5.1 Acquisition of cracks in GFRP Specimens

Successful acquisition of crack geometry depends on multiple important variables such as lighting, camera resolution, surface quality of specimen edges, material transparency, etc., from which the most important variables identified in this research were surface quality of specimen edges and lighting. As already stated in chapter 4.2 a comparison of classical micrography approach, custom grinding method and a customized milling process have been compared.

It is particularly important to acquire specimen sides for Prepreg materials, as many of the cracks are slanted and can be improperly classified by crack counting algorithms or experimenters resulting in false

determination of crack density. Prepreg materials show cracks that spread transversely through the specimen in an almost vertical manner up to the point where slanted cracks start to appear. In textile specimens the cracks are first, briefly, retarded by the weft yarns only to later coalesce and form larger cracks, which then spread transversely through the specimen. Figure 6 shows the comparison of cracking in specimens fabricated by different processing methods.

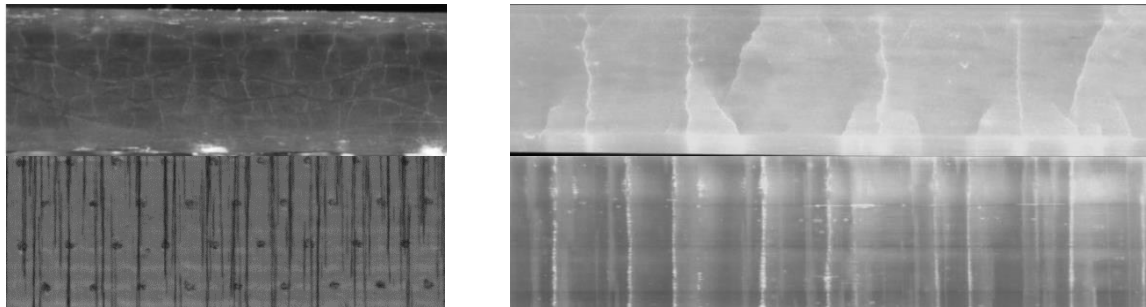


Figure 6 left: cracking in a textile specimen; right: cracking in a prepreg specimen

6 Conclusions

6.1 First simulation results

A virtual specimen containing 15 and later 41 cracks was simulated using ABAQUS XFEM. Stiffness degradation of the specimen with 41 cracks showed a good correlation with the experiment. At this time, no degradation was enabled in the outer 0° layers, which resulted in virtual tests showing greater residual strength than in the experiment. Although the XFEM method has been found to be a good choice for crack propagation simulation, some numerical difficulties related to its implementation in ABAQUS still exist. Further, it is not possible to define a crack that has more than two branches and the coalescence of two cracks shows an unrealistic behaviour.

Due to good correlation of residual stress-strain curves between real and virtual tests, it can be concluded that this methodology has potential to significantly shorten the time required to conduct residual strength testing, enabling the engineer a simplified framework for life prediction of composite structures. Figure 7 shows the stress-strain diagrams of 15 and 41 cracks virtual specimens compared to a real specimen.

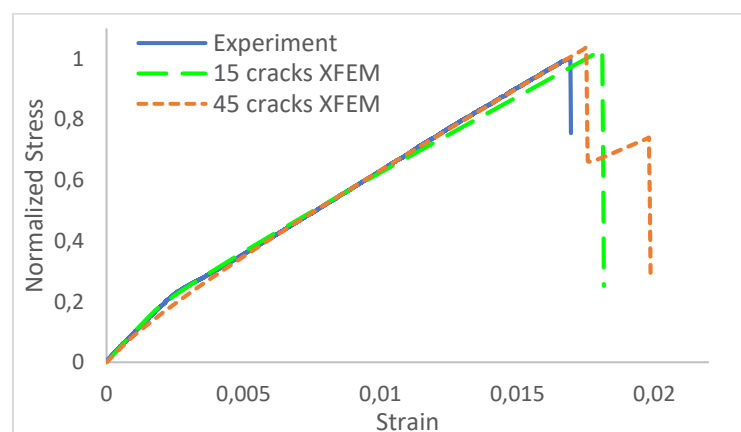


Figure 7 Comparison of simulation results with the experiment

6.2 Acquisition and crack detection

The current algorithm has shown that good crack detection is possible by using available image processing algorithms. Currently, the system is able to detect up to 70% of acquired cracks. Due to the

complexities of surface texture around the crack, detection of smaller cracks still remains a difficult task for the algorithm.

7 Next steps and future work

Several points require further attention. The investigation of the influence of specimen shape on cracking behaviour is an important topic to be addressed. The image processing algorithm needs to be further developed in order to be able to detect smaller cracks. Use of computer-vision and deep learning algorithms can facilitate this, and is currently under development. Finally, the simulation model will be updated to include 3D cracking and degradation of 0° layers.

8 Acknowledgements

The presented work has been conducted as part of the following grant-aided programme: “Forschungsbrücke Karlsruhe – Stuttgart” supported by the Ministerium für Wissenschaft, Forschung und Kunst Baden-Württemberg.

9 References

- [1] J. Degrieck and W. Van Paepegem, “Fatigue damage modeling of fibre-reinforced composite materials: Review,” *Appl. Mech. Rev.*, vol. 54, no. 4, pp. 279–300, Jul. 2001.
- [2] A. P. Vassilopoulos, Ed., *Fatigue life prediction of composites and composite structures / edited by Anastasios P. Vassilopoulos*. Boca Raton : Oxford: CRC Press ; Woodhead Publishing, 2010.
- [3] P. C. Chou and R. Croman, “Residual Strength in Fatigue Based on the Strength-Life Equal Rank Assumption,” *Journal of Composite Materials*, vol. 12, no. 2, pp. 177–194, Jul. 1978.
- [4] N. L. Post, “Reliability based design methodology incorporating residual strength prediction of structural fiber reinforced polymer composites under stochastic variable amplitude fatigue loading,” Virginia Polytechnic Institute and State University, 2008.
- [5] N. L. Post, J. Cain, K. J. McDonald, S. W. Case, and J. J. Lesko, “Residual strength prediction of composite materials: Random spectrum loading,” *Engineering Fracture Mechanics*, vol. 75, no. 9, pp. 2707–2724, Jun. 2008.
- [6] J. R. Schaff and B. D. Davidson, “Life Prediction Methodology for Composite Structures. Part I—Constant Amplitude and Two-Stress Level Fatigue,” *Journal of Composite Materials*, vol. 31, no. 2, pp. 128–157, Jan. 1997.
- [7] R. P. L. Nijssen, “Fatigue life prediction and strength degradation of wind turbine rotor blade composites,” s.n.], S.l., 2006.
- [8] A. P. Vassilopoulos and T. Keller, *Fatigue of Fiber-reinforced Composites*. London: Springer London, 2011.
- [9] J. A. Glud, J. M. Dulieu-Barton, O. T. Thomsen, and L. C. T. Overgaard, “Automated counting of off-axis tunnelling cracks using digital image processing,” *Composites Science and Technology*.
- [10] S. van der Walt *et al.*, “scikit-image: image processing in Python,” *PeerJ*, vol. 2, p. e453, Jun. 2014.
- [11] N. Otsu, “A Threshold Selection Method from Gray-Level Histograms,” *IEEE Transactions on Systems, Man, and Cybernetics*, vol. 9, no. 1, pp. 62–66, Jan. 1979.
- [12] U. Ramer, “An iterative procedure for the polygonal approximation of plane curves,” *Computer Graphics and Image Processing*, vol. 1, no. 3, pp. 244–256, Nov. 1972.